

# Colloid-polymer mixtures in the protein limit

Peter G. Bolhuis\*, Evert Jan Meijer\* and Ard A. Louis†

\*Dept. of Chemical Engineering, University of Amsterdam,  
Nieuwe Achtergracht 166, 1018 WV, Amsterdam, Netherlands

†Dept. of Chemistry, University of Cambridge, Lensfield Road, CB2 1EW, Cambridge, UK

(Dated: February 1, 2008)

We computed the phase-separation behavior and effective interactions of colloid-polymer mixtures in the “protein limit”, where the polymer radius of gyration is much larger than the colloid radius. For ideal polymers, the critical colloidal packing fraction tends to zero, whereas for interacting polymers in a good solvent the behavior is governed by a universal binodal, implying a constant critical colloid packing fraction. In both systems the depletion interaction is not well described by effective pair potentials but requires the incorporation of many-body contributions.

PACS numbers: 82.35.Np, 61.25.Hq, 82.70.Dd

Adding polymers to suspensions of micro- and nanoparticles induces depletion interactions that profoundly affect their physical properties. This phenomenon has important scientific and (bio-)technological applications. Polymers such as polyethylene glycol are routinely added to protein solutions to enable protein crystallization [1, 2], a poorly understood process and of great importance in structural biology [3]. In cell biology depletion interactions are key in the process of macro-molecular crowding [4]. Food and paint production are among the industrial sectors where depletion phenomena play a role.

In this Letter we focus on mixtures of hard sphere (HS) colloids with a radius  $R_c$  and non-adsorbing polymers with a radius of gyration  $R_g$ , in the regime where  $q = R_g/R_c > 1$ . This is often called the nano-particle or “protein limit”, because in practice small particles such as proteins or micelles are needed to achieve large size-ratios  $q$ . Whereas the opposite “colloid limit” ( $q \lesssim 1$ ) has been well studied, the physics in the protein limit is less established. This imbalance is partially due to the lack of well characterized experimental model systems for the protein limit and partially to a poor theoretical understanding. The colloid limit can be well described within the framework of effective depletion pair potentials [5, 6], in contrast to the protein limit, where the interactions cannot be reduced to a pairwise form [7, 8]. Nevertheless, for biological and industrial applications, this regime is at least as important as the colloid limit.

One of the first theoretical treatments of colloid-polymer mixtures in the protein limit was by de Gennes [9], who showed that the insertion free-energy  $F_c^{(1)}$  of a single hard, non-adsorbing sphere into an athermal polymer solution scales as

$$\beta F_c^{(1)} \sim (R_c/\xi)^{3-1/\nu} \quad (1)$$

when  $R_c < \xi$ , with the polymer correlation length  $\xi(\phi_p) \sim R_g \phi_p^{-\nu/(3\nu-1)} \approx R_g \phi_p^{-0.77}$  [10]. Here,  $\beta = 1/k_B T$  is the reciprocal temperature,  $\nu \approx 0.59$  is the Flory exponent and  $\phi_p = \rho_p \frac{4}{3} \pi R_g^3$  is the polymer volume fraction for a polymer number density  $\rho_p$ , so that

$\phi_p \approx 1$  at the crossover from a dilute to a semi-dilute solution [10]. The prefactors can be calculated by the renormalization group (RG) theory [11], yielding:  $\beta F_c^{(1)} \approx 4.39 \phi_p q^{-1.3}$  which has been verified by computer simulations for small  $q$  [12]. Based on this description of  $F_c^{(1)}$ , de Gennes [10] and Odijk [8] predicted extensive miscibility for colloid-polymer mixtures in the large  $q$  limit if  $R_c < \xi$ . However, it is well known that protein-polymer mixtures do phase-separate [13, 14]. Recently, Odijk *et al.* [15] suggested that a poor solvent could facilitate phase-separation. Sear [16] altered the form of  $F_c^{(1)}$  to include effects when  $R_c \gg \xi$ , and also predicted phase-separation with a truncated virial theory. The same author recently proposed an alternative theory [17] where the colloids induce depletion attractions between the polymers, leading to a poorer effective solvent and eventually phase-separation. Mean-field cell model calculations also predict demixing [18]. Another promising approach uses integral equation techniques [19] to predict spinodal curves and critical points. However, all these theories suffer from several uncontrolled approximations leading to different predictions for the causes and properties of the phase-separation. To clarify this situation, we performed computer simulations with as few simplifying assumptions as possible, on which we report in this Letter.

We have recently used a coarse-graining technique [20] to study the colloid limit, and found quantitative agreement with experimental fluid-fluid binodals [21], and significant qualitative differences between interacting (IP) and non-interacting (NIP) polymers. Here, we study the same athermal model of HS colloids and non-adsorbing polymers in the protein limit, and calculate, for the first time, the full fluid-fluid binodals by direct simulation. The results for the IP and NIP show even larger qualitative differences, and many-body depletion interactions must be invoked to understand the phase-behavior.

The simulation model consists of polymers on a simple cubic lattice mixed with HS colloids. The interacting polymers in a good solvent are modeled as self avoid-

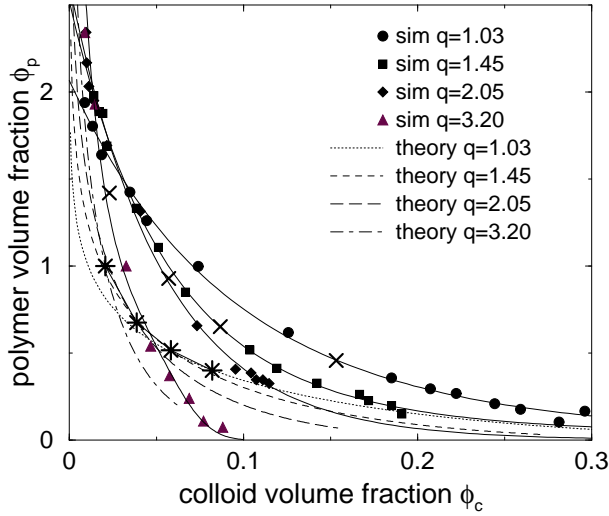


FIG. 1: Fluid-fluid binodals for a mixture of non-interacting polymers and HS colloids with different size-ratios  $q$ . Crosses indicate the estimated critical point, obtained by extrapolating the calculated phase boundaries. The full lines are a guide to the eye. Dashed lines denote the simple theory described in the text, with stars marking the critical points.

ing walks (SAW) of length  $L$ , which have a radius of gyration  $R_g \sim L^\nu$ . The non-interacting polymers are modeled as random-walks, for which  $R_g \sim L^{0.5}$ . In both models there is an excluded-volume interaction between the colloidal HS and the polymer segments. The simulations were performed on a  $D^3$  lattice with periodic boundary conditions, where  $D = 48$  and  $D = 100$  for the NIP and IP system, respectively. Throughout this Letter, we use the lattice spacing as the unit of length. For the NIP the colloidal HS diameter was  $\sigma_c = 5.5$  and the polymer length was  $L = 50, 100, 200$  and  $500$ , corresponding to  $q = 1.03, 1.45, 2.05$  and  $3.2$ , respectively. For the IP  $L = 2000$ , and  $\sigma_c = 10, 14$  and  $20$ , yielding  $q = 3.86, 5.58$  and  $7.78$ , respectively. Colloidal positions have continuous values, but when we calculated the interaction between colloid and polymer the colloids were shifted such that they occupied a constant number of lattice sites to prevent spurious attractive positions for single colloids (other lattice effects, although unavoidable, are expected to be small.) Thermodynamic state points were calculated in the grand-canonical ensemble, i.e. at fixed volume  $V$ , colloid chemical potential  $\mu_c$  and polymer chemical potential  $\mu_p$  using Monte Carlo (MC) techniques. The NIP were sampled using an (exact) lattice propagation method [22, 23], while the IP configurations were generated using translation, pivot moves and configurational bias MC [24] in an expanded ensemble to facilitate insertion of long chains [25]. Typical simulations lengths are  $10^9$  Monte Carlo moves per state point. In order to determine the liquid-liquid binodals we first estimated the coexistence line by scanning a series of  $\mu_c$

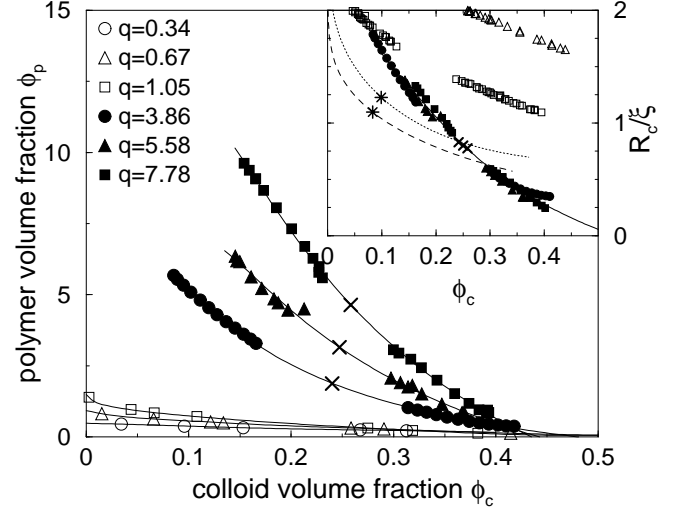


FIG. 2: Fluid-fluid binodals for a mixture of interacting polymers and HS colloids at different size-ratios  $q$ . Filled symbols are direct simulation data. The open symbols are the colloid limit ( $q \lesssim 1$ ) results from Ref. [21]. Solid lines are a guide to the eye. Inset: The same binodals plotted in a reduced polymer density representation. The dotted curve corresponds to a simple theory for the universal binodal when polymers are in a good solvent while the dashed line is for polymers in a poorer solvent. Crosses and stars as in Fig. 1.

for several values of  $\mu_p$  and locate the  $\mu_c$  for which a sudden density change occurred. Subsequently 8-10  $(\mu_p, \mu_c)$  coexistence state points were simulated simultaneously using parallel tempering [25]. When the estimated coexistence points are sufficiently close to the true binodal and to each other, and near the critical point, this scheme results in proper ergodic sampling of both phases. If necessary, the chemical potentials were adjusted towards coexistence. We used the multiple histogram reweighting [25, 26] technique to determine the precise location of the  $(\mu_c, \mu_p)$  coexistence line, and the phase boundaries in the  $(\phi_c, \phi_p)$  plane, where  $\phi_c = \rho_c \frac{4}{3} \pi R_c^3$  is the colloid volume fraction, with  $\rho_c$  the colloid number density.

Figs. 1 and 2 contrast the calculated phase diagrams for NIP and IP for several size-ratios  $q$ . Firstly, we note that both models show extensive immiscibility, in agreement with experiment [14]. Secondly, the two systems exhibit striking differences: for the NIP, the critical colloid volume fraction  $\phi_c^{crit}$  tends to zero with increasing size-ratio  $q$ , while the IP exhibit a nearly constant value of  $\phi_c^{crit}$ . For both systems the critical polymer concentration  $\phi_p^{crit}$  increases with increasing  $q$ . The phase-separation occurs well into the semi-dilute regime for the IP, again in qualitative agreement with experiment [13]. Properties of semi-dilute polymer solutions are independent of polymer length, being instead determined by the correlation length  $\xi$ , which is a function of the monomer density  $c = L\rho_p$ . The phase behavior of the polymer-HS mixture

should therefore only be a function of the ratio  $R_c/\xi$  [16]. Indeed, when the phase lines in Fig. 2 are rescaled with an accurate prescription for  $\xi(\rho_p)$  [12], the binodals nearly collapse onto a “universal binodal”, as shown in the inset of Fig. 2. This explains why the critical colloid packing fraction is nearly constant in the simulations. Similarly,  $\phi_p^{crit}$  scales as  $\phi_p^{crit} \sim q^{(3\nu-1)/\nu} \approx q^{1.3}$ . For comparison, we have also included results for  $q \lesssim 1$  from Ref. [21] in Fig. 2. These results do not exhibit the same scaling behavior, since they are not in the semi-dilute regime.

The differences between NIP and IP phase behavior can be rationalized with some simple theories. Consider a Helmholtz free-energy  $F$  of the form  $\beta F/V = f = f_c^{HS} + f_p + f_{cp}$ . Here, the HS free energy  $f_c^{HS}$  is given by the accurate Carnahan-Starling expression [27], and the polymer free energy  $f_p$  for either IP or NIP solutions is well understood [10]. The contribution due to the HS-polymer interactions  $f_{cp}$  is non-trivial. A first approximation truncates after the second cross-virial coefficient, yielding  $f_{cp} \sim \rho_c F_c^{(1)}$ . For NIP the insertion free-energy  $F_c^{(1)}$  is exactly known [11], so that  $f_{cp}$  takes the form  $f_{cp}^{id} = \rho_p \phi_c \left(1 + \frac{6q}{\sqrt{\pi}} + 3q^2\right) \equiv \rho_p \phi_c \hat{b}_{cp}$ , which defines the reduced cross-virial coefficient  $\hat{b}_{cp}$ . Since  $f_{cp}^{id}$  grows with increasing  $q$ , immiscibility sets in at lower colloid packing fraction  $\phi_c$ . The theory can be improved by realizing that the polymers only exist in the free volume left by the colloids [28]. Simply taking this free volume to be  $1 - \phi_c$  is an adequate first approximation for the protein limit. The trends for the binodal lines calculated from this simple theory, shown in Fig. 1, agree qualitatively with the simulations. For example, the critical point shifts to smaller  $\phi_c$  and larger  $\phi_p$  for increasing  $q$ , and the binodal lines cross at a low  $\phi_c$ . For computational reasons the simulations only go up to  $q = 3.2$  and we expect better quantitative agreement for larger  $q$  since  $\phi_c^{crit}$  decreases so that the second-virial theory should become more accurate. In the  $q \rightarrow \infty$  limit, this theory yields  $\phi_c^{crit} \rightarrow 1/\hat{b}_{cp} \sim 1/(3q^2)$ , and  $\phi_p^{crit} = q^3/\hat{b}_{cp} \sim q/3$ . Note that in the same limit, the penetrable sphere or Asakura-Oosawa model [28] scales somewhat differently:  $\phi_c^{crit} \rightarrow 1/q^3$  and  $\phi_p^{crit} \rightarrow 1$ . Sear [7] already pointed out the  $\phi_c^{crit} \rightarrow 0$  behavior using a slightly different prescription for the free volume than we employ here. Here we claim that the limiting results are a general feature of free-volume theories.

In the IP case,  $f_{cp}$  is more difficult to estimate, even for a second cross-virial theory. The  $R_c \ll \xi$  limit is given by Eq. (1) with the prefactors from RG theory. For  $R_c \geq \xi$  we have previously shown that  $F_c^{(1)}$  is given by  $F_c^{(1)} = \frac{4}{3}\pi R_c^3 \Pi + 6\pi R_c^2 \gamma_s$  [12], where the polymer osmotic pressure  $\Pi \sim \xi^{-3}$  is well known [10]. However, since Eq. (1) is essentially a surface (depletion layer) contribution, we use a simple approximate second cross-virial term  $f_{cp} = \rho_c (\beta \Pi(\rho) \frac{4}{3}\pi R_c^3 + 4.39\phi_p q^{-1.3})$ , which

reduces to the correct form in both the  $R_c \ll \xi$  and the  $R_c \gg \xi$  limit [33]. As with our treatment of NIP, we take the effect of the colloid excluded volume into account by computing the polymer densities in the free volume fraction  $1 - \phi_c$  (see Ref. [29] for a complimentary approach). The theoretical binodals were calculated using accurate expressions for  $\xi$  and  $\Pi$  [12] and are compared with the simulation results in Fig. 2, in the  $R_c/\xi$  versus  $\phi_c$  plane. The qualitative agreement suggests that we can also use this theory to estimate the effect of a poorer solvent on the binodals. Following Ref. [15], we alter the scaling of  $\xi$  to  $\xi \sim \phi_p^{-\delta/3}$  so that  $\Pi \sim \xi^{-3} \sim \rho_p \phi_p^{\delta-1}$ . Interestingly, Fig. 2 shows that using  $\delta \sim 1.5$  instead of the appropriate exponent for polymers in a good solvent ( $\delta \sim 2.3$ ), does not result in important differences in the binodals. Of course, the differences will appear larger in the  $(\phi_c, \phi_p)$  plane due to the different scaling of  $\xi$ . One must keep in mind, however, that these predictions follow from a simple scaling theory and qualitatively different behavior may emerge when one approaches the  $\theta$ -point (where  $\delta = 1$ ).

To illustrate the many-body nature of the depletion interaction we estimated the phase behavior by approximating the system by colloids interacting via pairwise effective potentials. We computed the effective pair interaction  $v(r)$  between two colloids in a bath of IP's, by  $\beta v(r) = -\ln g(r)$  for  $\rho_c \rightarrow 0$ . The colloid radial distribution function  $g(r)$  was estimated by measuring the insertion probability of a HS at a distance  $r$  from a second fixed HS in a SAW polymer solution using the above MC techniques. Results for a single size-ratio  $q = 7.78$  as a function of  $\phi_p$  are shown in Fig. 3. Several features are

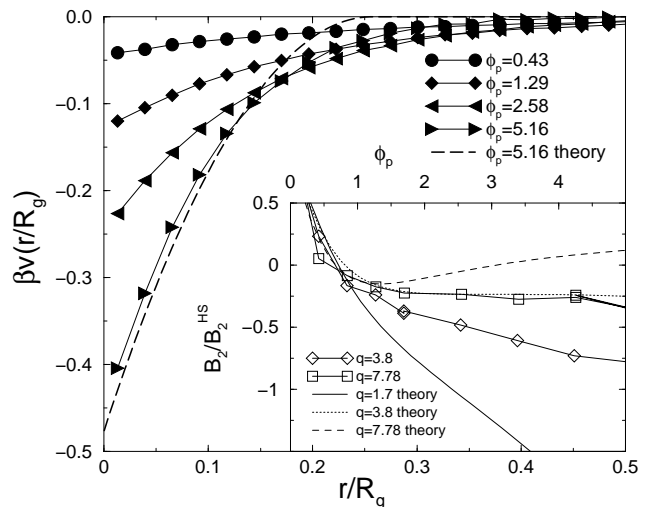


FIG. 3: Effective colloid-colloid pair potentials induced by interacting polymers for  $q=7.78$ . Theoretical lines from Ref. [30]. Inset: Reduced second osmotic virial coefficient  $B_2^* = B_2/(\frac{2}{3}\pi R_c^3)$  as a function polymer densities for several size ratio's.

similar to the colloid limit [30]: the range shortens and the well-depth increases with increasing  $\phi_p$ . Interestingly, our simple depletion potential [30], derived for the colloidal limit, also works semi-quantitatively in this regime. A good measure for the attractive strength of an effective pair potentials is given by the second osmotic virial coefficient [27], shown in Fig. 3. The saturation of  $B_2^*$  for larger  $q$  is an interesting qualitative feature: apparently the shortening of the range compensates the deepening of the attraction, so that the total cohesion does not increase with increasing  $\phi_p$ , something also found in RG [11] and integral equation calculations [19]. For pairwise interacting systems, phase-separation typically sets in when  $B_2^* \leq -1.5$  [31]. Here, the saturation of  $B_2^*$  suggests that for large  $q$  the pair interactions do not provide enough cohesion to explain the phase-separation. We arrive at the same conclusions with simple mean-field theories [27], which should be relatively trustworthy given the long range of the pair potentials. Obviously, for  $q \gg 1$  a pair-level description is not sufficient, and many-body interactions must be invoked.

For the NIP, one might also expect many-body interactions to be important for large  $q$ . A good approximation to the pair-potentials exists [23, 30], from which the second virial coefficients at the calculated critical points follow:  $B_2^*(q = 1.03) \approx -13.1$ ;  $B_2^*(q = 1.45) \approx -16.4$ ;  $B_2^*(q = 2.05) \approx -22.7$ . Even though the actual critical  $\phi_c$ 's are very low, so that a second-virial description might be thought to be sufficient, the analysis above shows that for NIP the pair-interactions provide too much cohesion, *opposite* to the IP case. Clearly, many-body interactions must also be invoked to describe the phase-behavior correctly, as suggested by other authors [7, 8, 19, 23, 32].

In conclusion, we have shown by computer simulations that a mixture of polymers and non-adsorbing HS colloids shows extensive immiscibility in the protein limit, where the polymer-colloid size-ratio  $q \gg 1$ . For IP the phase-behavior is dictated by a universal binodal in the semi-dilute regime. For NIP, the colloid packing fraction tends to zero for increasing polymer length. In contrast to the better studied colloid limit, pair interactions are not sufficient to rationalize the phase behavior. We hope that future experiments on HS colloids with non-adsorbing polymer will test these predictions. Future work might include extensions to non-spherical particles, poor solvents, and adsorbing systems.

A.A.L. acknowledges the Isaac Newton Trust for financial support. E.J.M. acknowledges the Royal Netherlands Academy of Art and Sciences for financial support. We acknowledge support from the Stichting Nationale Computerfaciliteiten (NCF) and the Nederlandse Organisatie voor Wetenschappelijk Onderzoek (NWO) for the use of supercomputer facilities. We thank M. Fuchs, R. Sear

and R. Tuinier for helpful discussions.

- 
- [1] A. M. Kulkarni *et al.*, Phys. Rev. Lett. **83**, 4554 (1999); J. Chem. Phys. **113**, 9863 (2000).
  - [2] S. Tanaka and M. Ataka, J. Chem. Phys. **117**, 3504 (2002).
  - [3] S.D. Durbin and G. Feher, Annu. Rev. Phys. Chem. **47**, 171 (1996).
  - [4] S.B. Zimmerman and A.P. Minton, Annu. Rev. Bioph. Biom. **22**, 27 (1993).
  - [5] S. Asakura and F. Oosawa, J. Chem. Phys. **22**, 1255 (1954).
  - [6] See W. C. K. Poon, J. Phys.: Condens. Matter **14**, R859 (2002) for a recent review.
  - [7] R.P. Sear, Phys. Rev. Lett **86** 4696 (2001).
  - [8] T. Odijk J. Chem. Phys. **106** 3402 (1997).
  - [9] P.G. de Gennes, C. R. Acad. Sci., Paris B **288**, 359 (1979).
  - [10] P.G. de Gennes, *Scaling Concepts in Polymer Physics*, (Cornell University Press, Ithaca).
  - [11] E. Eisenriegler *et al.*, Phys. Rev. E **54**, 1134 (1996); E. Eisenriegler, J. Chem. Phys. **113**, 5091 (2000).
  - [12] A.A. Louis, P.G. Bolhuis, J.P. Hansen, and E.J. Meijer, J. Chem. Phys. **116**, 10547 (2002).
  - [13] R. Tuinier *et al.*, Langmuir **16**, 1497 (2000).
  - [14] For a review see e.g. J.-L. Dublier *et al.*, Curr. Opin. Colloid In. **5**, 202 (2000).
  - [15] S. Wang *et al.*, Biomacromolecules **2**, 1080 (2001).
  - [16] R.P. Sear, Phys. Rev. E **56**, 4463 (1997).
  - [17] R.P. Sear, preprint, cond-mat/0206320.
  - [18] H.M. Schaink and J.M. Smit, J. Chem. Phys **107**, 1004 (1997).
  - [19] M. Fuchs and K.S. Schweizer, Europhys Lett. **51**, 21 (2000); J. Phys.: Condens. Matt. **14**, R239 (2002).
  - [20] A.A. Louis *et al.*, Phys. Rev. Lett. **85**, 2522 (2000); P.G. Bolhuis *et al.*, J. Chem. Phys. **114**, 4296 (2001).
  - [21] P.G. Bolhuis *et al.*, Phys. Rev. Lett. **89** 128302 (2002).
  - [22] D. Frenkel, J. Phys.: Condens. Matter **2**, SA265 (1990).
  - [23] E.J. Meijer and D. Frenkel, Phys. Rev. Lett. **67**, 1110 (1991); J. Chem. Phys. **100**, 6873 (1994).
  - [24] D. Frenkel and B. Smit, *Understanding molecular simulations, 2nd ed.* (Academic Press, San Diego, 2002).
  - [25] Q. Yan and J. J. de Pablo, J. Chem. Phys. **113**, 1276 (2000).
  - [26] A. M. Ferrenberg and R. H. Swendsen, Phys. Rev. Lett. **61**, 2635 (1987).
  - [27] J.P. Hansen and I.R. McDonald, *Theory of Simple Liquids, 2nd Ed.* (Academic Press, London, 1986).
  - [28] H.N.W. Lekkerkerker *et al.*, Europhys. Lett. **20**, 559 (1992).
  - [29] D. G. A. L. Aarts *et al.*, J. Phys.: Condens. Matter **14**, (2002).
  - [30] A.A. Louis *et al.*, J. Chem. Phys. **117**, 1893 (2002).
  - [31] G. A. Vliegenthart and H. N. W. Lekkerkerker, J. Chem. Phys. **112**, 5364 (2000).
  - [32] A.P. Gast, C.K. Hall and W.B. Russel, J. Colloid Interf. Sci. **96**, 251 (1983).
  - [33] Obviously this approach, which resembles the more schematic theory of Sear [16], could be improved.